Genetic manipulation of adult mouse neurogenic niches by *in vivo* electroporation

Fanie Barnabé-Heider[1], Konstantinos Meletis[1,4], Malin Eriksson[1], Olaf Bergmann[1], Hanna Sabelström[1], Michael A Harvey[2], Harald Mikkers[1,3] & Jonas Frisén[1]

Targeted ectopic expression of genes in the adult brain is an invaluable approach for studying many biological processes. This can be accomplished by generating transgenic mice or by virally mediated gene transfer, but these methods are costly and labor intensive. We devised a rapid strategy that allows localized *in vivo* transfection of plasmid DNA within the adult neurogenic niches without detectable brain damage. Injection of plasmid DNA into the ventricular system or directly into the hippocampus of adult mice, followed by application of electrical current via external electrodes, resulted in transfection of neural stem or progenitor cells and mature neurons. We showed that this strategy can be used for both fate mapping and gain- or loss-of-function experiments. Using this approach, we identified an essential role for cadherins in maintaining the integrity of the lateral ventricle wall. Thus, *in vivo* electroporation provides a new approach to study the adult brain.

The development of transgenic animal technology[1] and viral vectors[2,3] has made it possible to modulate gene expression within the adult brain *in vivo*. Although these techniques have advanced our understanding of the brain immensely, the associated labor and financial costs limit their use. Acute virus-mediated gene delivery is faster and can circumvent compensatory mechanisms frequently seen in transgenic animals, but many viral vectors activate the host's immune response, potentially interfering with the process being studied.

The availability of most genes in expression plasmids, combined with the possibility of specific suppression of gene expression by RNA interference, has triggered enormous interest in the development of new nonviral gene-based therapies in humans[4,5]. Cell transfection can be accomplished *in vitro* with one of several chemical reagents. Transfection reagents have been adapted for use *in vivo*, but they have not come into general use owing to toxicity and low efficiency[6]. The application of an electrical field to cells (electroporation) results in the transient and reversible formation of pores when the voltage across the plasma membrane exceeds its dielectric strength, allowing uptake of DNA. Electroporation is a commonly used transfection method *in vitro* and in some tissues *in vivo*[7]; and *in utero* electroporation has become a valuable approach in developmental neurobiology[8,9].

Here we present a rapid and efficient strategy for localized gene transfer into the adult mouse brain *in vivo* by electroporation. This method allows transfection of a variety of cell types without apparent damage and enables genetic gain- and loss-of-function experiments. Targeting the lateral ventricle and the hippocampus, we demonstrated that electroporation enables ectopic gene expression and genetic recombination in neural stem or progenitor cells and neurons. Moreover, using this method, we showed that the cadherin family of cell adhesion molecules is required for the integrity of the adult lateral ventricle wall.

RESULTS

Efficient gene transfer by electroporation in adult brain

We injected plasmid DNA into the lateral ventricle and delivered a train of electroporation pulses with electrodes held to the surface of the anesthetized mouse's head. This resulted in efficient plasmid uptake and gene expression (**Fig. 1a**). Transfection was not limited to the injected lateral ventricle; it was also efficient in the contralateral lateral ventricle as well as in the third ventricle (**Fig. 1a**).

As electric fields pull the negatively charged DNA toward the cathode, it is possible to direct the transfection to a specific part of the ventricle wall by altering the position of the electrodes (**Fig. 1b**,**c**). We detected expression from transfected plasmids within 36 h, and expression was detectable for up to 4 weeks (described below). Simultaneous injection of two plasmids encoding GFP and DsRed resulted in >99% coexpression (**Fig. 1d**), and simultaneous injection of three plasmids encoding GFP, DsRed and Cre resulted in 98% coexpression (**Fig. 1e**,**f**).

We tested several parameters to optimize targeting efficiency. A voltage ramp experiment from 50–300 V showed that plasmid uptake and expression occurred only at voltages greater than 200 V (**Supplementary Fig. 1a** online). The optimal injection time was 0.5–1 min/μl, and electroporation should be performed 1–2 min after retraction of the needle (**Supplementary Fig. 1b**). Using these

[1]Department of Cell and Molecular Biology, Medical Nobel Institute and [2]Department of Neuroscience, Box 285, Karolinska Institutet, SE-171 77 Stockholm, Sweden. [3]Department of Molecular Cell Biology and Regenerative Medicine Program, Leiden University Medical Center, P.O. Box 9600, 2300 RC Leiden, The Netherlands. [4]Present address: The Picower Institute for Learning and Memory, Massachusetts Institute of Technology, 43 Vassar Street, Cambridge, Massachusetts 02139, USA. Correspondence should be addressed to J.F. (jonas.frisen@ki.se).

RECEIVED 27 SEPTEMBER 2007; ACCEPTED 13 DECEMBER 2007; PUBLISHED ONLINE 20 JANUARY 2008; DOI:10.1038/NMETH.1174

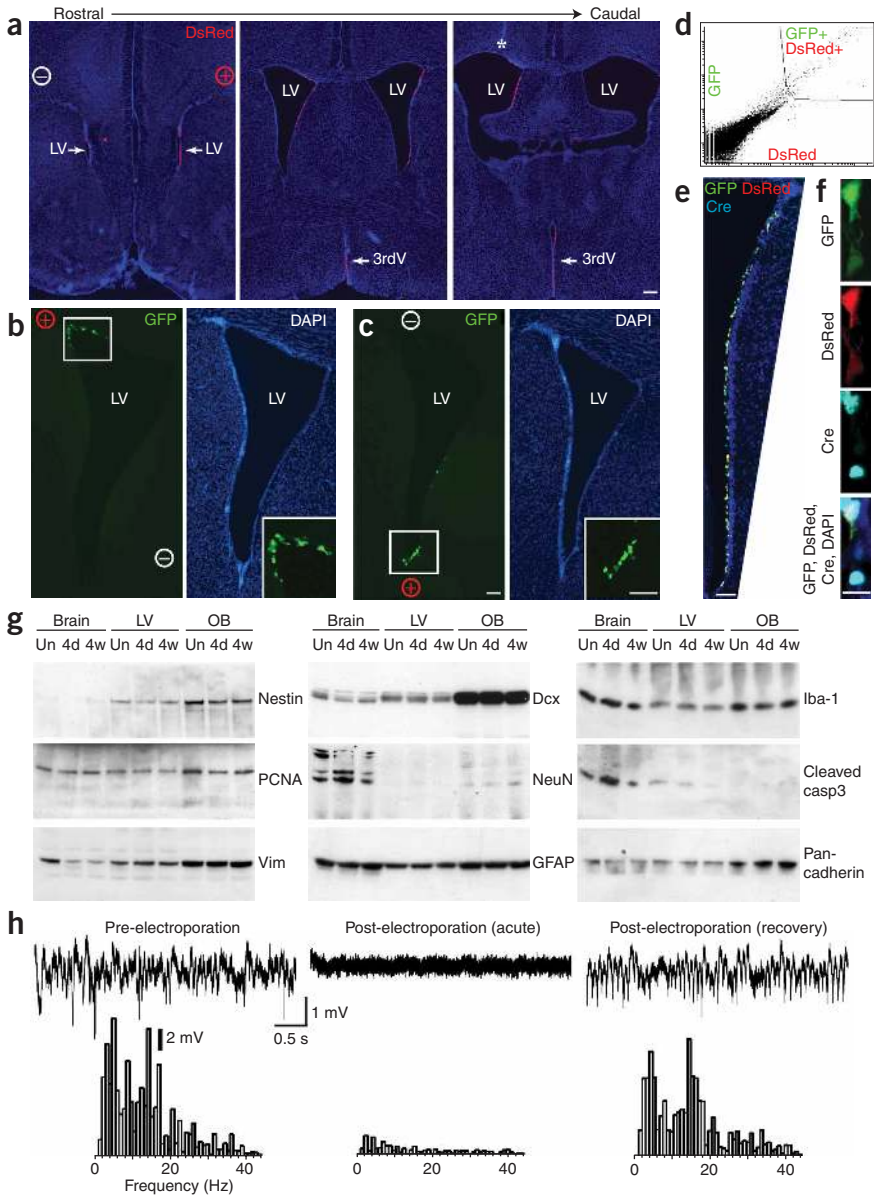

Figure 1 | Gene transfer to the adult brain without detectable damage by electroporation. (**a**–**f**) Analysis of lateral ventricle wall cells 5 d after injection and electroporation of expression plasmids. DsRed was efficiently expressed by cells along the rostrocaudal axis (**a**; >2 mm between the sections shown) within both the lateral (LV) and third (3rdV) ventricles. Asterisk, injection site. We achieved directional targeting to dorsal (**b**) or ventral (**c**) aspects of the lateral ventricle wall by positioning the electrodes (+, cathode; –, anode). Cells coexpress simultaneously electroporated plasmids (**d**–**f**), as shown by FACS analysis for GFP and DsRed (**d**), and by immunostaining for GFP, DsRed and Cre (in **e**, and at higher magnification in **f**). (**g**) Western blot analysis of different brain regions did not show any apparent differences in markers of neural lineage (nestin, PCNA, vimentin (Vim), Dcx and GFAP), markers of differentiated cells (NeuN and GFAP) or markers of injury (GFAP, Iba-1, cleaved caspase-3 (casp3), pan-cadherin) between untreated (Un) and electroporated brains after 4 d or 4 weeks (4w). OB, olfactory bulb; LV, lateral ventricle wall; Brain, remaining brain lysate. (**h**) Representative intrahippocampal local field potential recordings (top) and their respective power spectra (bottom) before and immediately after electroporation, and after recovery from electroporation. Sections were counterstained with 4,6-diamidino-2-phenylindole (DAPI) to show all nuclei. Scale bars, 100 μm (**a**–**c**,**e**) and 25 μm (**c** inset, **f**).

conditions and a high-purity DNA preparation, transfection was successful in nearly all mice. The efficiency was proportional to the DNA concentration injected and ranged from 20–30 to 50–70 transfected cells per section, on average, for DNA concentrations of 10 μg/μl and 20 μg/μl, respectively (average from 5–10 sections randomly distributed through the rostrocaudal axis; $n = 3$).

Electroporation does not cause detectable damage

We next asked whether the electroporation of DNA caused damage to the brain. In both vehicle- and DNA-injected mice that were electroporated, histological examination did not uncover any sign of damage except for the expected slight gliosis along the injection track. We did not find any evidence of inflammatory reaction, change in cell proliferation or alteration in the number of neuroblasts in the neurogenic niche (**Supplementary Fig. 1c**–**e**). This was markedly different from mice that received an injection of the transfection reagent polyethyleneimine, which showed prominent and widespread gliosis around the ventricle (data not shown). As an additional test for damage, we performed western blot analysis using a panel of markers for cell types or proteins associated with an injury response. In the lateral ventricle area of the microdissected olfactory bulb (of which the ependyma and subventricular zone form ~10%; **Supplementary Fig. 1f**) and in the remainder of the brain, this test did not identify any differences between untreated mice and mice subjected to electroporation (**Fig. 1g**). Moreover, the conditions used for electroporation did not induce seizures, and mice did not show any signs of burns or other reactions at the locations of the electrodes. Intrahippocampal electroencephalographic (EEG) recordings showed stereotypical theta oscillations before the initiation of the electroporation protocol, followed by depressed local field potential records for a period ranging between 30 min and 1 h ($n = 3$ mice). After 1–2 h, all mice had largely recovered a normal EEG pattern, measured both in terms of visual inspection and by the representative peaks in the power spectrum at 5 Hz and 14 Hz. From 2–6 h after electroporation, the hippocampal local field potential records were indistinguishable from control values (**Fig. 1h**). There was no increased lethality among mice that were subjected to electroporation compared to mice that received an intraventricular injection alone (>95% survival 2 d to 4 weeks after electroporation).

General and cell type–specific gene expression

We used cell type–specific markers to characterize the transfected cells in the lateral ventricle wall. Ependymal cells, which line the

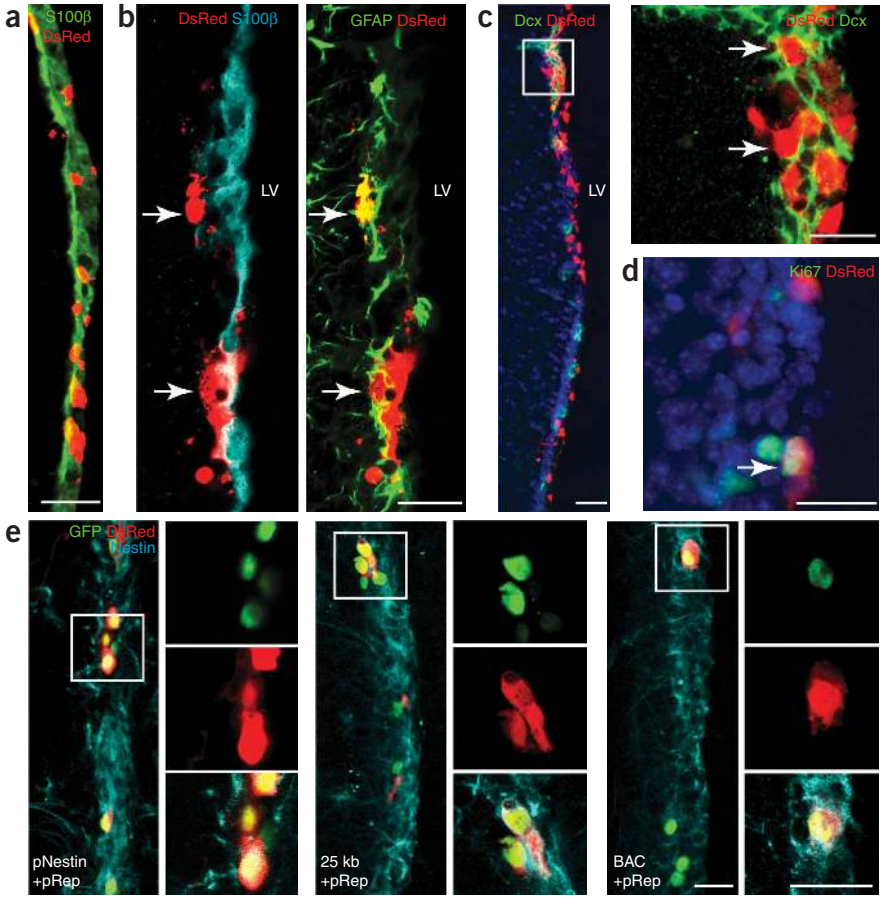

Figure 2 | Cell types targeted by electroporation in the lateral ventricle wall. (**a**–**d**) Analysis of brains 5 d after injection and electroporation of DsRed expression plasmid into the lateral ventricle. The majority of transfected cells were S100β$^+$ ependymal cells (**a**), but GFAP$^+$ astrocytes (**b**), Dcx$^+$ neuroblasts (**c**) and Ki67$^+$ proliferating cells (**d**) were also targeted. The outlined area in **c** is shown at higher magnification at right; arrows indicate double-positive cells. (**e**) Restricted expression results from electroporation of plasmids expressing Cre driven by a nestin enhancer (left), a 25-kb truncated version of the nestin promoter (center) or a 125-kb BAC containing the full nestin promoter (right). Cre expression was monitored by co-electroporation of a reporter plasmid (pRep) encoding a nuclear GFP and a Cre-dependent cytoplasmic DsRed. The expression of both GFP and DsRed in the same cell may be due to perdurance of GFP protein or incomplete recombination. For each set of panels, high-magnification images of the outlined area are shown at right. All sections were counterstained with DAPI. Scale bars, 50 μm (**a**,**c** (left)) and 25 μm (**b**,**c** (right), **d**,**e**).

ventricle, were the most efficiently transfected (**Fig. 2a**). However, in contrast to viral delivery of DNA, which usually is limited to ependymal cells[2,10,11], plasmid DNA was also expressed by cells in the subventricular zone of the lateral ventricle 36 h and 5 d after electroporation, including by glial fibrillary acidic protein–positive (GFAP$^+$) putative neural stem or progenitor cells (5.6% and 3.9% of transfected cells, respectively), Ki67$^+$ proliferating cells (2% and 2.6%, respectively) and doublecortin-positive (Dcx$^+$) neuroblasts (0.8% and 1.1%, respectively; **Fig. 2b–d**; percentages represent an average from four to six sections from three mice for each time point). Thus, electroporation allows gene transfer not only to ependymal cells but also to some adjacent cells in the subventricular zone.

We next tested whether we could target gene expression to a subpopulation of cells. Using a minimal nestin enhancer to drive Cre recombinase expression, we were able to restrict recombination efficiently to nestin-positive cells, as monitored by co-electroporation of a reporter plasmid (pRep) that switches from expression of nuclear GFP to DsRed expression upon Cre-mediated recombination. We observed ubiquitous nuclear GFP expression, but DsRed expression was restricted to nestin-positive cells (the latter is shown in **Fig. 2e**). Notably, it was also feasible to direct gene expression to nestin-positive cells when using larger 25-kb and 125-kb (**Fig. 2e**) DNA constructs containing nestin flanking sequences and a cDNA encoding Cre recombinase inserted at the transcription initiation site.

Transfection of neurogenic cells in the adult ventricle wall

The successful transfection of candidate neural stem or progenitor cells and neuroblasts by electroporation (**Fig. 2**) suggested that it may be possible to transfect cells in the neurogenic lineage in the adult lateral ventricle wall. This would be valuable for experimental purposes, and targeting of such cells may also be an attractive therapeutic approach[12]. In order to test directly whether cells giving rise to neurons in the adult brain could be transfected, we electroporated a plasmid encoding Cre recombinase in Z/EG[13] or R26R (ref. 14) mice, in which cells stably and heritably express a reporter gene (GFP in Z/EG and LacZ in R26R) upon recombination. Analysis of the lateral ventricle wall 4 weeks later showed recombined cells both in the ependymal layer and in the subventricular zone (**Fig. 3a**), demonstrating that at least some of the transfected cells are stationary nonmigrating cells. Many of these cells were still Cre$^+$, indicating persistence of the plasmid and continued gene expression (71.7% ± 11.6% Cre$^+$ cells; average from five sections containing 40–50 total GFP$^+$ cells per mouse; $n = 3$; **Fig. 3a**,**b**). However, there were also recombined cells that did not express Cre in the lateral ventricle wall and in the rostral migratory stream (RMS), the migratory path for neuroblasts *en route* to the olfactory bulb (**Fig. 3a**,**b**). Moreover, some of the recombined cells in the subventricular zone were Dcx$^+$ neuroblasts (**Fig. 3a**,**b**). As this is a transient and migratory cell phenotype, the presence of recombined neuroblasts 4 weeks after the transfection indicated that long-term neurogenic stem or progenitor cells had been transfected and that they were continuing to produce genetically labeled progeny.

Analysis of the olfactory bulb showed the presence of recombined cells both in the center, where the RMS enters, as well as in the granular cell layer (**Fig. 3c–f**). The recombined cells in the core of the olfactory bulb were all Dcx$^+$ (**Fig. 3c**,**d**), whereas the

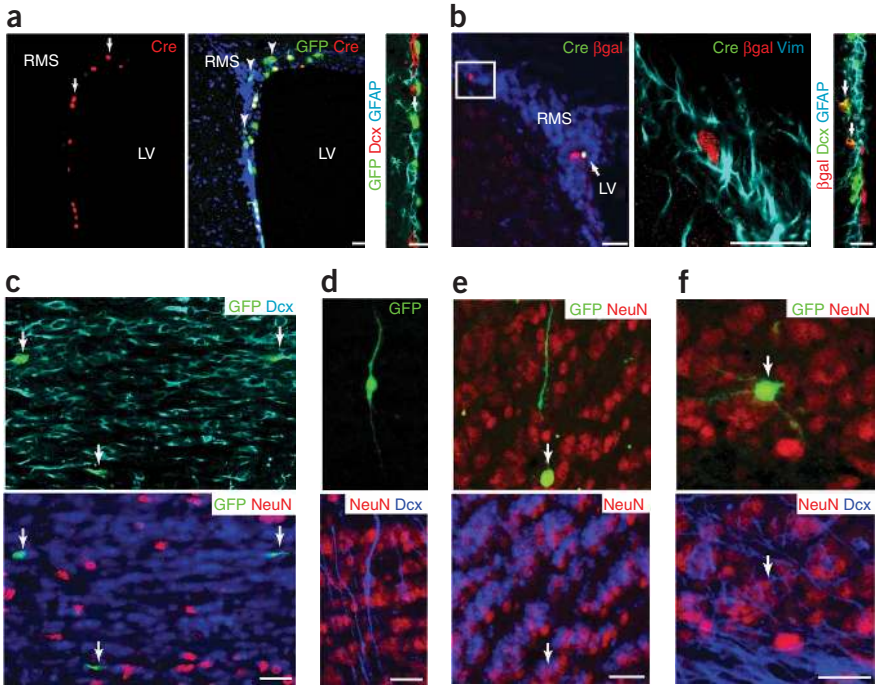

Figure 3 | Electroporation targets cells with neural stem cell properties. (**a**–**f**) Analysis of cells from the lateral ventricle 4 weeks after injection and electroporation of Cre plasmid in the lateral ventricle in either Z/EG (**a**,**c**–**f**) or R26R (**b**) reporter mice. Cre expression is either maintained by cells of the lateral ventricle wall (**a**, arrows, left panel) or lost by GFP$^+$ recombined cells (**a**, arrowheads, center panel). Some GFP$^+$ recombined cells coexpress GFAP (**a**, arrow, right panel). Cre$^+$ cells in the lateral ventricle wall (**b**, arrow, left) give rise to Cre$^-$ β-gal$^+$ cells in the RMS (**b**, center panel, showing higher magnification of the outlined area at left). Some β-gal$^+$ recombined cells coexpress the neuroblast marker doublecortin (Dcx; **b**, arrows, right panel). Recombined cells derived from the lateral ventricle wall are found in the RMS (**c**) and are Dcx$^+$ neuroblasts negative for the mature neuronal marker NeuN (arrows indicate recombined cells in **c**). (**d**–**f**) In the olfactory bulb, GFP$^+$ recombined cells integrate in the neuronal layers and are either Dcx$^+$ immature cells (**d**) or differentiated NeuN$^+$ neurons with elaborated processes (**e**,**f**). Arrows point to NeuN$^+$ recombined cells. Sections were counterstained with DAPI (**a**–**c**,**e**). Scale bars, 25 μm.

recombined cells in the granular layer showed the presence of NeuN, a marker for mature neurons, and had elaborate morphology with long branched processes (50% Dcx$^+$ and 50% NeuN$^+$, 1–6 cells per 20-μm section; average from 5 randomly distributed sections per mouse, $n = 3$; **Fig. 3e**,**f**). The presence of recombined cells of all maturational stages in the neurogenic lineage indicates the transfection of long-term neural stem or progenitor cells. Moreover, when we subjected Z/EG mice to electroporation with a nestin enhancer–driven Cre expression plasmid, neurosphere cultures from these mice gave rise to recombined, GFP$^+$ neurospheres 5 d later (data not shown).

Gene transfer to neurogenic cells in the adult hippocampus

The dentate gyrus of the hippocampus constitutes a second neurogenic niche in the adult brain[15]. We next asked whether electroporation would allow gene transfer not only after injection into the fluid-filled ventricles, but also after injection directly into the hippocampal parenchyma.

Electroporation in combination with injection of a plasmid solution directly into the vicinity of the dentate gyrus resulted in a highly localized patch of cells expressing the plasmid-encoded gene (**Fig. 4**). Probably because of the high cell density in this tissue, the vast majority of transfected cells were located within the

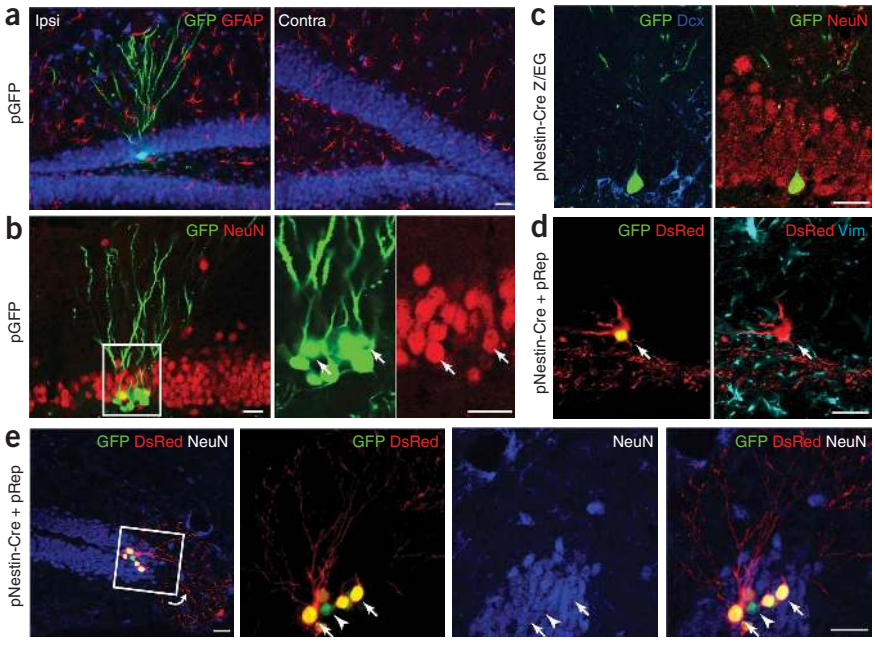

Figure 4 | Targeting the hippocampal neurogenic niche by electroporation. (**a**,**b**) Analysis of cells in the dentate gyrus 1 week after injection and electroporation of a plasmid encoding GFP. GFP$^+$ cells in the injected side (**a**, ispilateral, left) are found away from (~600 μm) the injected area. The number and morphology of GFAP$^+$ reactive astrocytes are comparable to those on the contralateral side (**a**, right), and transfected cells include NeuN$^+$ neurons (**b**, arrows). (**c**–**e**) Analysis of cells from the dentate gyrus 2 weeks after injection and electroporation of nestin-driven Cre plasmid (pNestin-Cre). In **c**, injection in Z/EG reporter mice leads to GFP$^+$ recombined neurons (like this one) that are negative for the neuroblast marker Dcx (left) but NeuN$^+$ (right). (**d**,**e**) Co-electroporation with the pRep reporter plasmid in wild-type mice shows targeting of immature vimentin-positive precursor cells (**d**), which give rise to NeuN$^+$ neurons (**e**). The three rightmost panels in **e** show targeted cells that were already neurons (GFP$^+$ only, arrowhead) or neurons derived from nestin-positive cells (GFP and DsRed–positive, arrows). Sections were counterstained with DAPI (**a**). Scale bars, 25 μm.

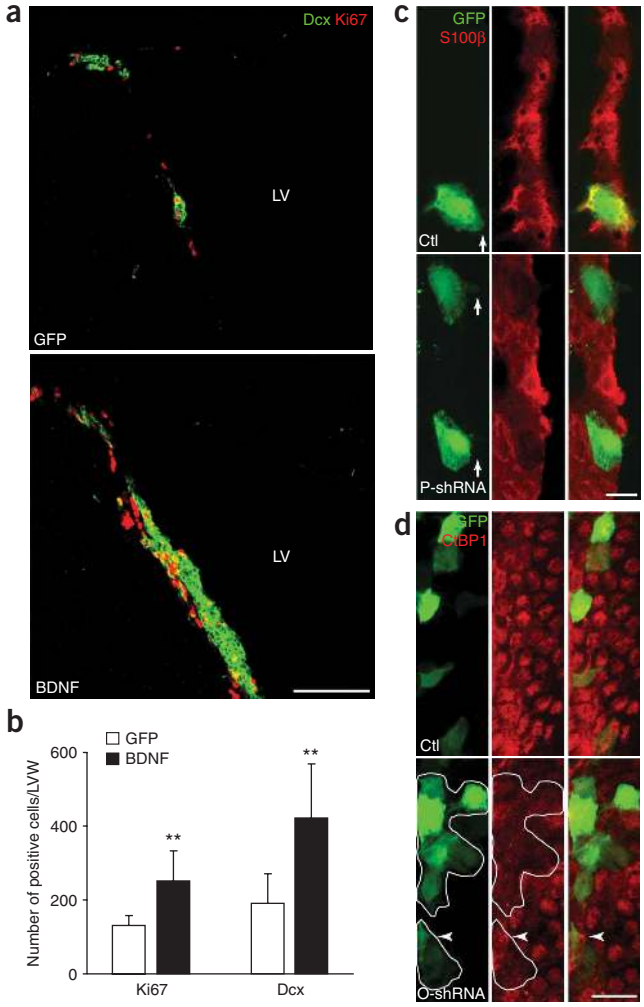

Figure 5 | Adult brain electroporation allows gain- and loss-of-function experiments. (**a**,**b**) Ki67$^+$ proliferating cells and Dcx$^+$ neuroblasts are significantly increased in number in the lateral ventricle (LV) wall upon BDNF expression (**a**, bottom) but not upon expression of a control plasmid encoding GFP (**a**, top; quantified in **b** (five sections per mouse)). $^{**}P < 0.01$, from three to five sections per mouse; $n = 3$ for each experimental group. (**c**) Analysis of GFP and S100β expression in cells located in the lateral ventricle wall 5 d after injection and electroporation of plasmids encoding GFP and either a scrambled shRNA sequence (Ctl) or shRNA against S100β (P-shRNA) and GFP. ShRNA expression leads to a marked reduction of S100β immunoreactivity in ciliated ependymal cells (arrows). (**d**) Analysis of CtBP-1 (a transcriptional corepressor expressed by ependymal and subventricular cells) expression in cells located in the lateral ventricle wall 36 h after injection and electroporation of GFP plasmid alone (top) or with oligonucleotide siRNA (O-shRNA) against CtBP-1 (bottom). The siRNA-transfected cells showed a marked reduction of staining (outlined area) in more than 75% of the GFP$^+$ cells (arrowhead points to a cell showing high expression of CtBP-1). Scale bars, 100 μm (**a**), 10 μm (**c**) and 20 μm (**d**).

subgranular and granular layer (**Fig. 4a–c**), and only rarely were cells located within the neuropil (**Fig. 4d**). Even though mature neurons are notoriously difficult to transfect, electroporation resulted in transfection of both NeuN$^+$ neurons within the granular cell layer (**Fig. 4b**,**c**) and immature vimentin-positive cells in the subgranular zone (**Fig. 4d**).

Electroporation of a nestin enhancer–driven Cre plasmid allowed specific targeting of neural progenitor cells in the subgranular zone (**Fig. 4d**,**e**). Transfection of this plasmid in the dentate gyrus allowed genetic recombination of the co-electroporated reporter plasmid pRep, which resulted in directly transfected neurons expressing only GFP and transfected newly born neurons derived from nestin-positive precursors expressing both GFP and DsRed (**Fig. 4e**). Thus, electroporation offers a new way to express genes in both neurogenic niches of the adult brain.

Genetic gain- and loss-of-function experiments

Ectopic gene expression can aid in the elucidation of gene function, and we next asked whether it was possible to influence cell phenotype or function by electroporating plasmid DNA in the adult brain. Brain-derived neurotrophic factor (BDNF) delivered by intraventricular infusion of recombinant protein or by adenoviral transduction of ependymal cells can prominently increase neurogenesis in the subventricular zone[16,17]. Electroporation of an expression plasmid encoding BDNF resulted in approximately twice as many proliferating cells and Dcx$^+$ neuroblasts in the treated mice compared to mice electroporated with a plasmid encoding GFP (**Fig. 5a**,**b**). Moreover, electroporation of oligonucleotides or plasmids encoding shRNA resulted in knockdown of target proteins as early as 36 h after electroporation (**Fig. 5c**,**d**). Thus, electroporation enables rapid gain- and loss-of-function studies in the adult brain.

An essential role for cadherins in an adult neurogenic niche

We next used the electroporation approach to ask whether the cadherin family of cell adhesion molecules is involved in maintenance of the adult lateral ventricle neurogenic niche, as was reported for other stem cell niches[18–20]. To confirm and further evaluate our results, we performed a parallel study using adenoviral expression. Both E- and N-cadherin are expressed most abundantly in ependymal cells in the adult lateral ventricle wall and at lower amounts in subventricular zone neuroblasts (**Fig. 6a**,**b** and **Supplementary Fig. 2a**,**b** online). To directly address the role of cadherins, we expressed a dominant-negative cadherin (DN-cadherin) by electroporation or using adenovirus (DN-cadherin also expresses a GFP-Cre fusion protein and therefore can be detected by staining for Pan-cadherin, N-cadherin or Cre or by GFP fluorescence; **Fig. 6c** and **Supplementary Fig. 3**)[21]. DN-cadherin is an N-terminally truncated version of human N-cadherin that suppresses expression of all cadherins, independent of isotype[21]. The DN-cadherin construct efficiently reduced endogenous cadherin amounts and reduced cell adhesion in *in vitro* assays without apparent toxicity (**Supplementary Fig. 2c–f**), as previously described[21]. Expression of DN-cadherin resulted in the detachment of ependymal cells after 2 d and was more pronounced after 5 d (**Fig. 6d**,**e** and **Supplementary Fig. 3a**). This resulted in a significant reduction in the number of DN-cadherin–expressing cells (**Fig. 6e**). The majority of the detaching cells did not show signs of cell death such as pyknotic nuclei or immunoreactivity to cleaved caspase 3 (**Supplementary Fig. 3b**), although there was a small increase in cell death upon DN-cadherin expression (**Fig. 6f**). We did not observe these phenotypes upon expression of a control construct (GFP plasmid and Cre adenovirus); here, the number of transfected cells remained constant after 5 d in an intact lateral ventricle wall (**Fig. 6d**,**e** and **Supplementary Fig. 3a**,**c**). At locations where ependymal cells were lost, aggregates of proliferating cells

formed polyp-like structures protruding into the ventricular lumen (**Fig. 6g** and **Supplementary Fig. 3c,d**; we observed 1–8 polyps for every 10 lateral ventricle wall sections analyzed; $n = 3$–4 for each group). The polyps contained proliferating (Ki67$^+$) cells with a neuroblast marker profile (Dcx$^+$, GFAP$^-$, vimentin-negative) but never contained DN-cadherin–positive cells (**Fig. 6g** and **Supplementary Fig. 3d**), suggesting that they arise as a secondary consequence of the loss of overlying ependymal cells. We conclude

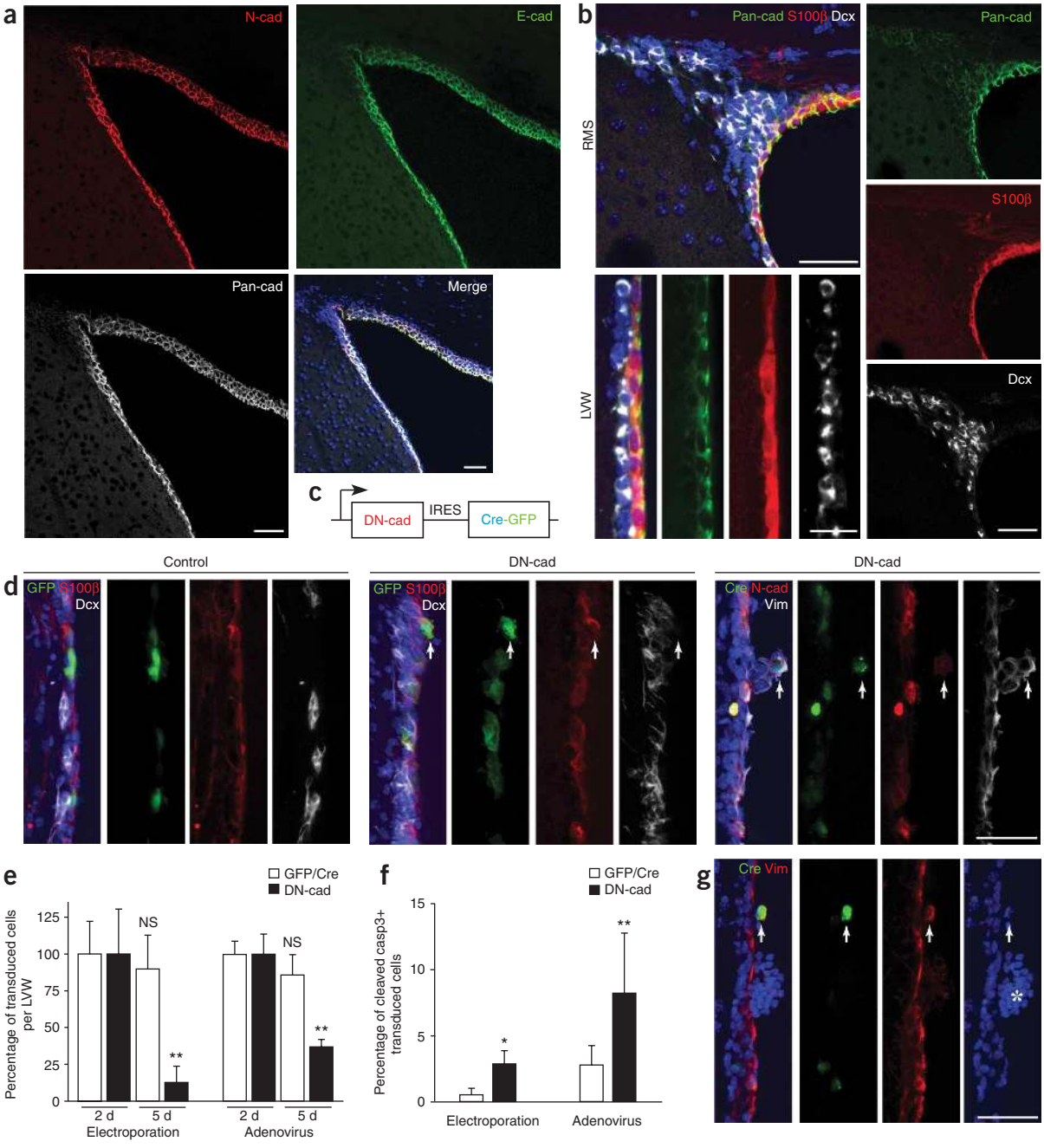

Figure 6 | Cadherins are essential for the integrity of the adult lateral ventricle wall. (**a**,**b**) Pan-cadherin and N- and E-cadherin are expressed in a similar pattern in the adult lateral ventricle wall (LVW) (**a**). They show the highest expression in S100β$^+$ ependymal cells and show lower expression in Dcx$^+$ neuroblasts (**b**). (**c**) Schematic of the DN-cadherin construct, in which the CMV promoter drives the expression of DN-cadherin, followed by a bicistronic IRES element upstream of the Cre-GFP fusion gene. (**d**) Expression of DN-cadherin (center and right) but not of control GFP (left) by electroporation resulted in disruption of the S100β$^+$ ependymal cell layer, and some cells detached from the ventricle wall (arrows) after 2 d. Note that endogenous cadherins are undetectable without antigen retrieval, whereas overexpressed DN-cadherin is readily detected, allowing visualization of transfected cells (right). (**e**) Quantification of the proportion of transduced cells remaining in the lateral ventricle wall after 5 d. The average number of transduced cells after 2 d was set to 100% ($n = 3$ for each group). (**f**) Quantification of the percentage of apoptotic (cleaved caspase3–positive) transduced cells 2 d after electroporation or adenoviral infection. (**g**) DN-cadherin electroporation results in the development of polyp-like structures (asterisk) containing vimentin-negative cells, which are bordered by, but do not contain, transduced cells (Cre$^+$). Arrows mark a detaching cell. Sections were counterstained with DAPI (**a**,**b**,**d**,**g**). Scale bars, 50 μm (**a**,**b** (RMS),**d**,**g**) and 20 μm (**b** (LVW)). $^*P < 0.05$, $^{**}P < 0.01$; NS, not significant; $n = 3$–4 for each experimental group.

that cadherins are essential for maintaining the integrity of the lateral ventricle wall.

Although the parallel study using adenoviral expression (**Supplementary Fig. 3**) gave similar results, electroporation offers a faster and more versatile method, in terms of both targeting several cell types (subependymal and ependymal cells) and directing transfection to specific regions (see legend of **Supplementary Fig. 3**). We conclude that the electroporation technique offers a rapid way to tackle biological questions in the adult brain.

DISCUSSION

The cost and labor associated with previously available methods for modulating gene expression *in vivo* have limited the speed of progress. A major advantage of electroporation compared to the generation of transgenic mice or viral vectors is speed; the amplification of an expression plasmid takes a few days, whereas the production of viral vectors and the establishment of mouse lines can take several weeks, months or years. Indeed, the same DNA construct that would be used to generate a transgenic mouse or a virus, as tested in the present study, can be delivered directly by electroporation. This becomes especially valuable when considering complex genetic experiments combining several transgenic mouse lines or viruses. Conditional gene manipulation (for example, with inducible Cre recombinase) is a powerful way to study gene function in mice[1]. However, it often calls for the establishment of double- or triple-transgenic mouse lines, and such studies are slow and costly owing to complex mouse breeding. We show that Cre expression can be achieved in promoter-defined cells, allowing temporal and spatial control of genetic recombination. This can be used to ablate genes or for genetic fate mapping, for example. Moreover, the fact that at least three plasmids can be delivered simultaneously by electroporation also allows complex genetic experiments without the need for mouse breeding, as recently shown in the postnatal retina[22].

The study of adult neurogenesis is important both for the understanding of normal brain function and for potential therapeutic relevance to human conditions such as stroke and depression[12,23]. The administration of plasmid DNA into the ventricular system allows efficient gene transfer to cells in the ventricle wall. Ependymal cells that are in direct contact with the ventricular lumen were the most efficiently transfected. However, in contrast to most viral strategies[2,10,11], subependymal cells were also targeted. There have been only a few attempts to target adult neurons *in vivo*, and these have used microelectrodes implanted into the brain parenchyma[24,25]. Here we demonstrate that externally applied electrodes can be used to target both newly born and mature neurons of the adult dentate gyrus by electroporation, avoiding the additional injury sites associated with electrode implantation.

The ependymal layer is an integral part of the adult lateral ventricle wall neurogenic niche. Numb and Numblike are required for maintaining the integrity of the lateral ventricle wall neurogenic niche, and the deletion of these genes results in reduction of E-cadherin and the detachment and loss of ependymal cells[26]. Numb and Numblike physically interact with cadherins *in vivo* and regulate adherens junction formation[26,27]. Thus, Numb and Numblike may maintain the integrity of the ependymal layer and the neurogenic niche by regulating cadherin function. However, Numb and Numblike are likely to control other functions, such as modulating the Notch signaling pathway. The specific role for cadherins in this context has not been assessed. We have used electroporation to test this hypothesis directly and have found that expression of a dominant-negative cadherin results in ependymal cell detachment, disruption of the ependymal layer and formation of polyps by neuroblasts protruding into the lateral ventricle. These findings provide evidence that cadherins are required for the integrity of this neurogenic niche.

Gene therapy in the human brain has been suggested as a potential future treatment for genetic diseases such as lysosomal storage disorders and for brain tumors[28]. Application of electrical current to the human brain is commonly used in electroconvulsive therapy for affective disorders. Although the electrical impulse settings differ, electroporation of adult brain cells *in vivo* does not lead to seizures or to detectable changes in neurogenesis or apoptosis, as has been reported upon brief and prolonged seizures[29]. Therefore, it is possible that electroporation of DNA could be considered for gene therapy for the treatment of human brain disorders.

METHODS

Adult brain electroporation and adenovirus injections. The Karolinska Institutet ethics committee approved all experiments. We deeply anesthetized adult C57BL/6 mice from Charles River and Z/EG[13] or R26R (ref. 14) reporter mice with Avertin (Sigma) and stereotaxically injected 2 µl (for the lateral ventricle) or 0.5 µl (for the dentate gyrus) of plasmid solution. The coordinates for injections in the lateral ventricle were AP 0.0; L 1.0; V –1.0 mm, and the coordinates for injections into the dentate gyrus of the hippocampus were AP –2.0; L 1.3; V –1.6 mm relative to Bregma. After injection, we applied conductive gel (Siemens) on the skin of the skull and electroporated using either square (1 cm × 1 cm, caliper electrode; VWR International) or round (0.5-cm diameter; TR Tech) electrodes and a square electroporator CUY21 EDIT (TR Tech) to deliver five 50-ms pulses of 200 V (the lowest voltage leading to transfected cells) with 950-ms intervals, which gives a voltage of about 100 V/cm and current of 0.2–0.3 A. We describe plasmids and their preparation in detail in **Supplementary Methods** online.

Immunohistochemistry. We transcardially perfused adult mice with PBS and then with 4% formaldehyde in PBS; we then post-fixed brains overnight at 4 °C and cut 30–40 µm sections using a vibratome. For some mice, we cryoprotected some olfactory bulbs and brains in 30% sucrose overnight before sectioning with a cryostat (30-µm sections). We describe the immunostaining procedure in **Supplementary Methods**. We obtained images using either a Zeiss Axioplan 2, Axiovert 200M or LSM510 META confocal microscope. We performed statistical analysis using pools of three to ten sections per mouse, with three to four mice per experiment. All graphs represent mean ± s.d.; we used Student's *t*-test to compare two groups.

Western blot analysis. We lysed and sonicated microdissected lateral ventricle walls, olfactory bulbs or remaining parts of the brain in radioimmunoprecipitation assay (RIPA) buffer. We washed HEK293 cells with PBS and harvested them in RIPA buffer 48 h after adenoviral infection. We separated equal amounts of protein by SDS-PAGE and transferred the separated proteins to nitrocellulose membranes. We describe the detection procedure in **Supplementary Methods**.

EEG recordings. We anesthetized the mice with Avertin and made a large craniotomy over the left cerebral hemisphere. We made local field potential recordings with bipolar tungsten electrodes constructed by joining two tungsten electrodes (FHC) together with dental acrylic in the CA1 hippocampal region (AP –2.0; L 1.5; V –1.5 mm relative to Bregma). Each electrode had a tip resistance of ~1 MΩ. Bipolar electrodes had vertical and horizontal separations of 0.1 mm and 0.2 mm, respectively. We amplified signals using a differential AC amplifier (AM Systems), digitized them with an A/D card (CED) and recorded results on a personal computer. We analyzed signals using Igor Pro (Wavemetrics) software.

Additional methods. We describe all plasmids, adenoviral constructs and antibodies used in the study, and give details on the immunohistochemical labeling and western blot detection procedures in **Supplementary Methods**.

Note: Supplementary information is available on the Nature Methods website.

ACKNOWLEDGMENTS

We thank R. Kageyama (Kyoto University) for the gift of the nestin promoter vector[30], C. Ibáñez (Karolinska Institutet) for the gift of a BDNF expression plasmid, M. Wheelock (University of Nebraska Medical Center) for providing the dominant-negative N-cadherin cDNA and K. Fernandes (University of Montreal) for critically reading the manuscript. This study was supported by grants from the Swedish Research Council, the Swedish Cancer Society, the Foundation for Strategic Research, the Karolinska Institutet, Tobias Stiftelsen and the European Commission Framework VI Programme, EuroStemCell. F.B.-H. is supported by a postdoctoral fellowship from Canadian Institutes of Health Research.

AUTHOR CONTRIBUTIONS

F.B.-H. designed, performed and analyzed the study and wrote the manuscript; K.M. designed and performed most parts of the study; M.E. performed and analyzed part of the study (including BAC analysis); O.B. performed part of the study; H.S. performed and analyzed part of the study; M.A.H. performed EEG analysis; H.M. designed and performed part of the adenoviral study; and J.F. designed the study and wrote the manuscript.

Published online at http://www.nature.com/naturemethods/
Reprints and permissions information is available online at http://npg.nature.com/reprintsandpermissions

1. Carlen, M., Meletis, K., Barnabe-Heider, F. & Frisen, J. Genetic visualization of neurogenesis. *Exp. Cell Res.* **312**, 2851–2859 (2006).
2. Consiglio, A. *et al.* Robust *in vivo* gene transfer into adult mammalian neural stem cells by lentiviral vectors. *Proc. Natl. Acad. Sci. USA* **101**, 14835–14840 (2004).
3. Tashiro, A., Zhao, C. & Gage, F.H. Retrovirus-mediated single-cell gene knockout technique in adult newborn neurons *in vivo*. *Nat. Protoc.* **1**, 3049–3055 (2006).
4. Glover, D.J., Lipps, H.J. & Jans, D.A. Towards safe, non-viral therapeutic gene expression in humans. *Nat. Rev. Genet.* **6**, 299–310 (2005).
5. Lu, P.Y., Xie, F. & Woodle, M.C. *In vivo* application of RNA interference: from functional genomics to therapeutics. *Adv. Genet.* **54**, 117–142 (2005).
6. Falk, A. *et al.* Gene delivery to adult neural stem cells. *Exp. Cell Res.* **279**, 34–39 (2002).
7. Mir, L.M., Moller, P.H., Andre, F. & Gehl, J. Electric pulse-mediated gene delivery to various animal tissues. *Adv. Genet.* **54**, 83–114 (2005).
8. Calegari, F., Haubensak, W., Yang, D., Huttner, W.B. & Buchholz, F. Tissue-specific RNA interference in postimplantation mouse embryos with endoribonuclease-prepared short interfering RNA. *Proc. Natl. Acad. Sci. USA* **99**, 14236–14240 (2002).
9. Inoue, T. & Krumlauf, R. An impulse to the brain–using *in vivo* electroporation. *Nat. Neurosci.* **4** (Suppl.), 1156–1158 (2001).
10. Bajocchi, G., Feldman, S.H., Crystal, R.G. & Mastrangeli, A. Direct *in vivo* gene transfer to ependymal cells in the central nervous system using recombinant adenovirus vectors. *Nat. Genet.* **3**, 229–234 (1993).
11. Johansson, C.B. *et al.* Identification of a neural stem cell in the adult mammalian central nervous system. *Cell* **96**, 25–34 (1999).
12. Falk, A. & Frisen, J. New neurons in old brains. *Ann. Med.* **37**, 480–486 (2005).
13. Novak, A., Guo, C., Yang, W., Nagy, A. & Lobe, C.G. Z/EG, a double reporter mouse line that expresses enhanced green fluorescent protein upon Cre-mediated excision. *Genesis* **28**, 147–155 (2000).
14. Soriano, P. Generalized lacZ expression with the ROSA26 Cre reporter strain. *Nat. Genet.* **21**, 70–71 (1999).
15. Kempermann, G., Jessberger, S., Steiner, B. & Kronenberg, G. Milestones of neuronal development in the adult hippocampus. *Trends Neurosci.* **27**, 447–452 (2004).
16. Benraiss, A., Chmielnicki, E., Lerner, K., Roh, D. & Goldman, S.A. Adenoviral brain-derived neurotrophic factor induces both neostriatal and olfactory neuronal recruitment from endogenous progenitor cells in the adult forebrain. *J. Neurosci.* **21**, 6718–6731 (2001).
17. Pencea, V., Bingaman, K.D., Wiegand, S.J. & Luskin, M.B. Infusion of brain-derived neurotrophic factor into the lateral ventricle of the adult rat leads to new neurons in the parenchyma of the striatum, septum, thalamus, and hypothalamus. *J. Neurosci.* **21**, 6706–6717 (2001).
18. Gonzalez-Reyes, A. Stem cells, niches and cadherins: a view from *Drosophila*. *J. Cell Sci.* **116**, 949–954 (2003).
19. Zhang, J. *et al.* Identification of the haematopoietic stem cell niche and control of the niche size. *Nature* **425**, 836–841 (2003).
20. Lechler, T. & Fuchs, E. Asymmetric cell divisions promote stratification and differentiation of mammalian skin. *Nature* **437**, 275–280 (2005).
21. Nieman, M.T., Kim, J.B., Johnson, K.R. & Wheelock, M.J. Mechanism of extracellular domain-deleted dominant negative cadherins. *J. Cell Sci.* **112**, 1621–1632 (1999).
22. Matsuda, T. & Cepko, C.L. Controlled expression of transgenes introduced by *in vivo* electroporation. *Proc. Natl. Acad. Sci. USA* **104**, 1027–1032 (2007).
23. Lindvall, O. & Kokaia, Z. Stem cells for the treatment of neurological disorders. *Nature* **441**, 1094–1096 (2006).
24. Kondoh, T. *et al.* *In vivo* gene transfer into the periventricular region by electroporation. *Neurol. Med. Chir. (Tokyo)* **40**, 618–623 (2000).
25. Wei, F. *et al.* Calmodulin regulates synaptic plasticity in the anterior cingulate cortex and behavioral responses: a microelectroporation study in adult rodents. *J. Neurosci.* **23**, 8402–8409 (2003).
26. Kuo, C.T. *et al.* Postnatal deletion of Numb/Numblike reveals repair and remodeling capacity in the subventricular neurogenic niche. *Cell* **127**, 1253–1264 (2006).
27. Rasin, M.R. *et al.* Numb and Numbl are required for maintenance of cadherin-based adhesion and polarity of neural progenitors. *Nat. Neurosci.* **10**, 819–827 (2007).
28. Wong, L.F. *et al.* Lentivirus-mediated gene transfer to the central nervous system: therapeutic and research applications. *Hum. Gene Ther.* **17**, 1–9 (2006).
29. Bengzon, J., Mohapel, P., Ekdahl, C.T. & Lindvall, O. Neuronal apoptosis after brief and prolonged seizures. *Prog. Brain Res.* **135**, 111–119 (2002).
30. Hatakeyama, J. *et al.* Hes genes regulate size, shape and histogenesis of the nervous system by control of the timing of neural stem cell differentiation. *Development* **131**, 5539–5550 (2004).

Genetic manipulation of adult mouse neurogenic niches by *in vivo* electroporation

Fanie Barnabé-Heider, Konstantinos Meletis, Malin Eriksson, Olaf Bergmann, Hanna Sabelström, Michael A Harvey, Harald Mikkers & Jonas Frisén

Supplementary figures and text:

Supplementary Figure 1 Gene transfer parameters for *in vivo* adult brain electroporation without detectable effects on the neurogenic niches.

Supplementary Figure 2 Endogenous cadherin expression and validation of DN-cadherin plasmid and adenovirus.

Supplementary Figure 3 Suppression of cadherin levels leads to ependymal cell loss and polyp formation.

Supplementary Methods

Supplementary Figures

Supplementary Figure 1 Gene transfer parameters for *in vivo* adult brain electroporation without detectable effects on the neurogenic niches.

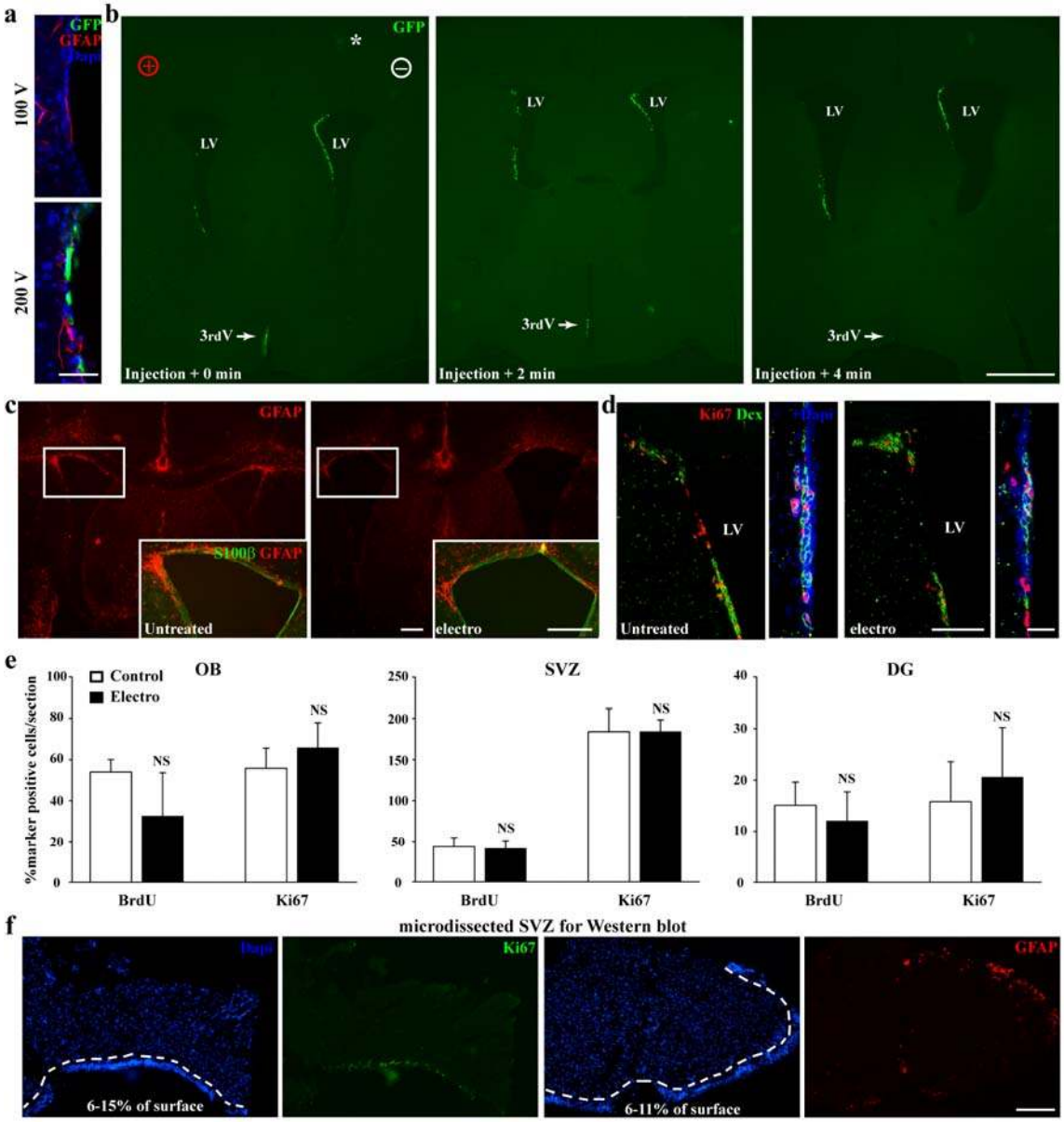

(**a**) Transfer and expression of a GFP plasmid is achieved following electroporation at a voltage of 200 V (lower panel) but not at 100 V (upper panel) without inducing gliosis ($GFAP^+$ astrocytes) in the neurogenic niche. (**b**) A GFP plasmid was injected and electroporated (orientation of the electrodes are marked by + for the cathode and – for the anode, and the injection site is marked with an asterisk) right after the injection (0 min) and after 2 or 4 min. Note that transfected cells are detectable in the 3rd ventricle shortly

after injection and that the efficiency is higher in the injected side at all time points, but that cells targeted to the contralateral side are fewer at 4 min. (**c,d**) Electroporation after two weeks does not result in gliosis and show undisrupted S100ß$^{+}$ ependymal layer (**c**) and electroporated brains show no apparent difference in the number or distribution of proliferating cells (Ki67) or neuroblasts (Doublecortin, Dcx) in the dorsal (left panels) or ventral (right panels) lateral ventricle neurogenic niche (**d**). (**e**) Injected only (control) and injected followed by electroporation (electro) animals received a single dose of BrdU immediately after the procedure. The total number of BrdU^{+} and Ki67^{+} cells within the subventricular zone of the hemisphere by the cathode were analyzed 5 days later in the rostral migratory stream entering the olfactory bulb (OB), the subventricular zone of the lateral ventricle (SVZ) and in the dentate gyrus of the hippocampus (DG) and showed no statistically significant difference (NS, n = 3-4 animals for each group, 3-5 sections per animal per area). (**f**) Microdissected ventricular areas (as used for Western blot analysis, see **Fig. 1g**) were fixed and cryostat sectioned. The SVZ and ependyma constituted in average 10% of the samples (marked by a dashed line) as revealed by Ki67 (2 left panels) and GFAP (two right panels) labeling. Sections were conterstained with Dapi (**a,c,d,f**). Scale bars are 50 μm (**a**), 1000 μm (**b**), 100 μm (**c,d** left panel), 25 μm (**d** right panel) and 200 μm (**f**).

Supplementary Figure 2 Endogenous cadherin expression and validation of DN-cadherin plasmid and adenovirus.

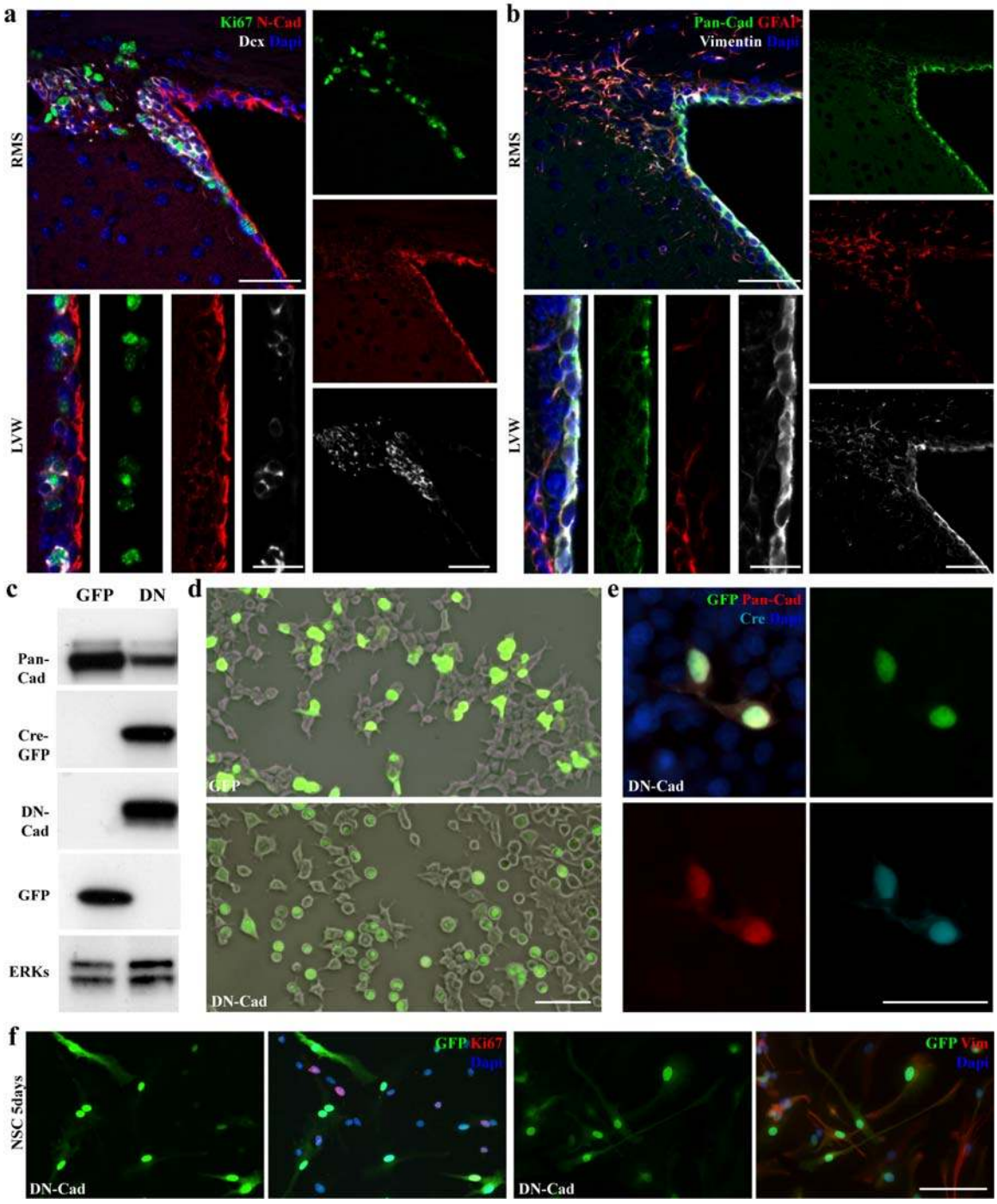

(**a,b**) Endogenous cadherin expression in the adult lateral ventricle wall neurogenic niche shows that N-cadherin is expressed at low levels in Ki67^{+} proliferating cells and in Dcx^{+} neuroblasts in comparison to ependymal cells (**a**). Pan-cadherin immunoreactivity is detected in vimentin^{+} ependymal cells lining the ventricle but not in GFAP^{+} astrocytes

(**b**). (**c,d**) HEK293 cells were infected with GFP or DN-cadherin adenovirus for 2 days. Western blot analysis shows expression of the fusion Cre-GFP, truncated N-cadherin and significant reduction of the endogenous full length cadherin proteins upon DN-cadherin infection. Antibody against ERKs was used to determine equal loading. (**c**) Live cell imaging shows that, whereas GFP infected cells grow in clusters and adhere to each others (**d**, top panel), DN-cadherin infected cells are less frequently found in clusters (**d**, bottom panel). (**e**) DN-cadherin plasmid was tranfected into HEK293 cells and shows co-expression of GFP, Pan-cadherin and Cre. (**f**) Dissociated neural stem cells from adult-derived neurospheres (NSC) were infected with DN-cadherin and analyzed 5 days later. GFP-positive infected cells are viable and some are $Ki67^+$ proliferating cells (left panels) and $vimentin^+$ precursor cells (right panels). Sections were conterstained with Dapi (**a,b,e,f**). Scale bars are 50 μm in SVZ and 20 μm in LVW (**a,b**), 100 μm (**d,f**), and 50 μm (**e**).

Supplementary Figure 3 Suppression of cadherin levels lead to ependymal cell loss and polyp formation.

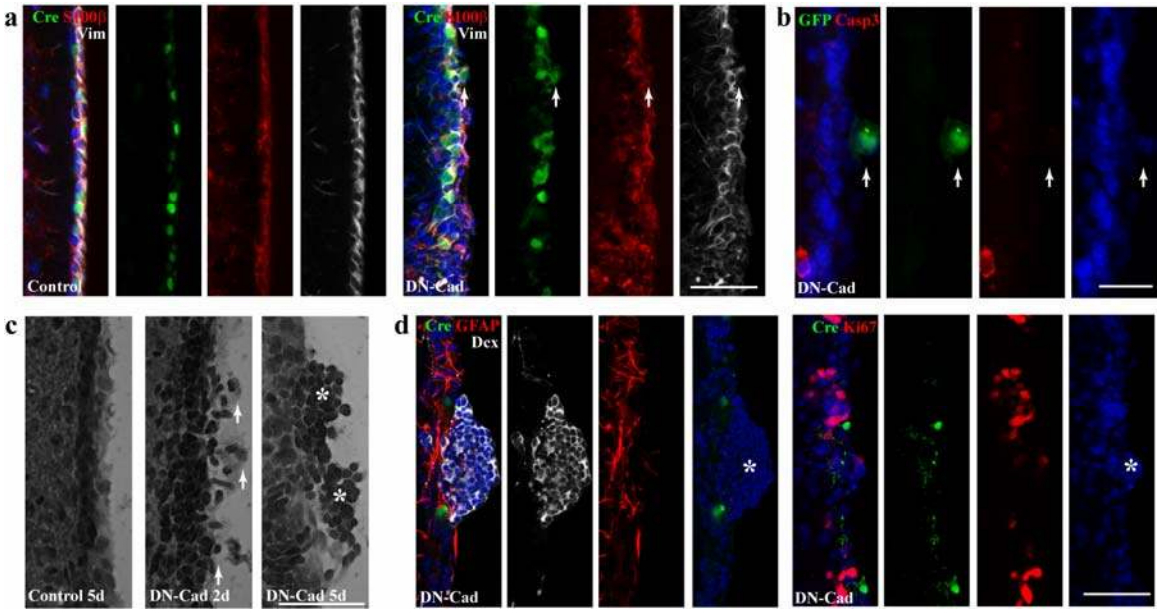

(**a-d**) Cadherin function was blocked either by injection of a DN-cadherin adenovirus derived from the electroporated plasmid (**a,c,d**) or by electroporation of DN-cadherin plasmid (**b**). Endogenous cadherins are undetectable without antigen retrieval whereas DN-cadherin readily is detected, allowing visualization of transduced cells. An adenovirus expressing Cre served as controls. DN-cadherin expression results in disruption of the layer of $S100\beta^+$ ependymal cells and some cells detach from the ventricle wall (arrow) after 2 days, as observed with electoporation. Of notice, adenoviral gene delivery results in a higher number of targeted cells but is restricted to ependymal cells. The mosaic distribution of electroporated cells allows the study of cell intrinsic component while being sufficiently robust to recapitulate the phenotype observed after adenovirus delivery or direct infusion of BDNF in the lateral ventricle (see **Fig. 5**). Moreover, electroporation allows targeting of a specific region (i.e. lateral versus medial or dorsal versus ventral, see **Fig. 1**) within the lateral ventricle, which is not feasible with an adenovirus-based approach. (**b**) Example of an electroporated DN-cadherin expressing cell (GFP^+, arrow), which is cleaved $caspase3^-$ (Casp3), is detaching from the wall. (**c,d**) DN-cadherin expression results in the development of polyp-like structures (asterisks). DN-cadherin expression leads to ependymal cells detachment from the wall after 2 days (arrows) and formation of polyps from non-ependymal cells as shown by H&E staining

(**c**). (**b**) Polyps contain $GFAP^-$, Dcx^+ and $Ki67^+$ cells that are bordered by, but do not contain, Cre^+ transduced cells (**d**). Sections were conterstained with Dapi (**a,b,d**). Scale bars are 50 μm (**a,c,d**,) and 20 μm (**b**).

Supplementary Methods

Plasmid and adenovirus preparation

The plasmids were prepared using a high purity maxiprep system (Marligen), resuspended in Tris buffer (10mM Tris HCl, pH 8.5) and were used at a final concentration of 5-20μg/μl. The plasmids used were: GFP (pCMV-EGFP-N1, Clontech), dsRed (pCMV-dsRed-express, Clontech), Cre, pNestin-Cre (Cre sequence was cloned into the nestin promoter vector[30], a kind gift of R. Kageyama), BDNF (from the AdMLP promoter, a kind gift of C. Ibáñez) and shRNA (U1promoter-driven S100β shRNA and GFP expression plasmids, Super Array Bioscience Corporation). The oligonucleotide-siRNA against CtBP1 (AMBION) was used at 50pMol/μl. The GFPcre-expressing BAC was constructed from a nestin locus-containing BAC (clone bMQ-370d01, Welcome Trust Sanger Institute), the 25kb nestinGFPcre vector was constructed by retrieval of 21kb including the GFPcre from the nestinGFPcre BAC, the cre-recombinase sensitive reporter vector pRep, pCALL2H3-GFPdsRed-express, was constructed from the pCALL2 vector (Clontech) where the cDNA of DsRed-express was cloned into the MCS and lacZ from the original vector replaced by a GFP. BAC electroporations were diluted in 50% nucleofection reagent (Amaxa).

The dominant negative N-cadherin cDNA (here referred as DN-cadherin), in which the cytosolic portion of human N-cadherin is N-terminally fused to the v-Src myristoylation sequence[21], was inserted into a modified pShuttle2 vector (Clontech) containing a bicistronic IRES element upstream of the CRE/GFP fusion gene. The pShuttle insert was either directly used for electroporation studies or was ligated into the pAdenoX vector (Clontech) according to the manufacturer's instructions and virus was generated by calcium phosphate mediated transfection of HEK293A cells with the pAdenoDN-cadherin plasmid. Subsequent amplification of the recombinant adenovirus was performed by ViraQuest Inc. The Cre adenonovirus was purchased from Microbix. Lateral ventricle injections were performed as mentioned above injecting 3-5μl of 10^{11} PFU adenoviral solution at a rate of 1μl/min.

Immunohistochemistry

Sections were incubated with blocking solution (10% donkey serum in PBS, with 0.3% Triton-X 100) for 1 hr, and incubated at 4°C or room temperature overnight with primary antibody diluted in blocking solution. For endogenous cadherin detection, antigen retrieval was performed boiling the mounted sections for 15 min in citrate buffer pH 6 prior to the blocking step. Primary antibodies directed against the following proteins were used: ß-gal (1:1000, rabbit, ICN-Cappel), doublecortin (1:1000, guinea pig, Chemicon), cleaved caspase3 (1:1000, rabbit, Cell Signaling), Cre (1:1000, mouse or rabbit, Nordic BioSite), CtBP1 (1:500, mouse, BD Pharmingen), E-cadherin (1:500, rat, Zymed), GFAP (1:1000, clone G-A-5, mouse, Sigma), GFP (1:500, rabbit or chicken, Chemicon), Ki67 (1:1000, rabbit, NeoMarkers), N-cadherin (1:500, mouse, Zymed), pan-cadherin (1:500, rabbit, Spring Bioscience), NeuN (1:500, mouse, Chemicon), nestin (1:2000, mouse, BD Pharmingen), S100ß (1:1000, rabbit, DAKO) and Vimentin (1:1000, chicken, Chemicon). After washing, antibody staining was revealed using species-specific fluorophore-conjugated secondary antibodies (Cy3, Cy5 from Jackson, Alexa 488 from Molecular Probes).

Western blot analysis

Membranes were blocked in 5% milk and incubated with the following antibodies overnight: cleaved caspase3 (1:1000, rabbit, Cell Signaling), Cre (1:2000, mouse, Nordic BioSite), Doublecortin (1:1000, rabbit, abcam), GFAP (1:5000, mouse, SIGMA), GFP (1:1000, rabbit, Chemicon), ERKs (1:5000, rabbit, Cell Signaling), Iba-1 (1:1000, rabbit, Wako), nestin (1:2000; mouse, BD Pharmingen), NeuN (1:1000, mouse, Chemicon), Pan-cadherin (1:5000, rabbit, Spring Bioscience), PCNA (1:1000, mouse, Santa Cruz), and Vimentin (1:5000, chicken, Chemicon). Membranes were then incubated with the appropriate HRP-conjugated secondary antibody (1:2000; Amersham Biosciences) in 5% milk and detection performed using ECL reagent and Hyperfilms (both from Amersham Biosciences).